BAUSTJ
BAUST Journal

A Review on Detection of Prostate Cancer Using Different Computer-Aided Diagnosis Techniques

SK Fahad As Sami[1*], Shad Bin Abi Aydid[2], Nabila Parvin[3], Asif Parvez Sarkar[4] and Md. Nakib Hayat Chowdhury[5]

[*1,2,3,4,5]Department of CSE, Bangladesh Army University of Science and Technology, Saidpur, Bangladesh

emails: [*1]*sami.baust.cse@gmail.com;* [2]*shadaydid@gmail.com;* [3]*nabilashayabaust@gmail.com;* [4]*asifparvezsarker26@gmail.com;* [5]*nakib@baust.edu.bd*

ARTICLE INFO

Article History:

Received: 9th September 2019
Revised: 25th July 2020
Accepted: 28th July 2020
Published online: 25th August 2020

Keywords:

Prostate Cancer CAD CNN GSM Image Processing MRI

ABSTRACT

One of the most frequently diagnosed cancer among males is prostate cancer (PC). The causes of PC are still unknown at the moment. In any event, a better understanding of the PC's ecology and genetic factors and their interaction will help physicians and patients in assessing individual PC hazards, and there will definitely be a chance to find a way to decrease the PC's development. There are many ways that prostate cancer can be detected. Likewise, for PC detection, magnetic resonance imaging (MRI), dynamic contrast-enhanced (DCE)-MRI, and diffusion-weighted imagery (DWI) were widely used. There are also non-invasive techniques that can detect the PC. The purpose of this paper is to provide an overview of non-invasive computer-aided diagnostic (CAD) techniques such as Image Processing, Convolution Neural Network (CNN), Graph Spectral Method (GSM), and other detection technique.

1. INTRODUCTION

Prostate cancer (PC) is a malignant (cancerous) tumor that begins in the prostate gland (PG) to progress. It is one of American males' most diagnosed cancer and the second major cause of cancer deaths in the US following lung cancer. Recent reports show that the number of newly diagnosed PC cases in 2018 is around 164,690 and the number of deaths is around 29,430. Men over the age of 50 are particularly vulnerable. PC has a rate of 70 percent. PC studies in individuals over 75 years of age were performed in Japan and the U.S. It is projected that the number of PC diagnoses will increase to 1,700,000 globally by 2030 and could be responsible for up to 500,000 deaths per year. Fortunately, in the event of early diagnosis of prostate cancer, the mortality rate may be reduced. The earlier a PC will be found, the more probable it will be a cure.

The likelihood of becoming affected is greater when a individual has a PC family history. The risk increases when the PC is owned by a relative of each additional first degree. Also, the individual who has an African origin has a greater risk of becoming impacted. An individual with deficiencies in vitamin D and E also has an opportunity to get impacted. Higher dietary fat and red meat eating also enhance the chance of affection. Keeping a healthy weight decreases the danger.

There are no symptoms in many instances, but as the phase of cancer progresses, some signs and symptoms begin to appear. Urinating difficulty, urgent need to urinate, frequent night urination, pain when urinating, urinary blood. If these symptoms appear in the early stages, the patient's survival is increased significantly. Using the tumor nodes and metastasis (TNM) system, PC grows locally within the prostate can be categorized into 4 stages. PC only exists in prostate at stage I and cannot be identified by prostate imaging. The tumor is still restricted to the prostate in phase II, but it has grown and can be identified through imaging. Prostate cancer

has started to spread outside the prostate in stage III. The cancer spread to other tissues in stage IV.

Prostate cancer's traditional diagnostic methods include assessment by digital rectal examination (DRE), prostate-specific antigen (PSA), and TRUS-guided biopsy. There are particular constraints to each of these methods. PSA is the most prevalent form of blood-based assessment currently used to detect prostate cancer. The primary issue of PSA screening is its elevated false positive and false negative rates as enhanced blood PSA concentrations may be due to prostate hyperplasia or inflammation. The use of PSA screening, however, led in a decrease of more than 20 percent of the mortality rate owing to prostate cancer.

In this paper, we use computer-aided diagnosis (CAD) to conduct a powerful literature review on the identification of prostate cancer. The first methods that use Image Processing, Convolutional Neural Network (CNN), Graph Spectral, and other detection techniques. Comparing them with Computer Aided Diagnosis (CAD) after that and trying to figure out which one is better.

2. LITERATURE REVIEW

Lung cancer is one of the most common causes of cancer death worldwide, estimated to account for nearly one in five (18.4% of the total, 1.76 million deaths).

Breast cancer is the second most prevalent cancer in the world, and the most recurrent number of fresh instances among females is around 11.6% and fatalities are around 6.6%, nearly one in fifteen.

Colon is another worldwide common cancer. The number of fresh instances is around 1.1 million and the amount of fatalities is around 5.9%, which is nearly one in seventeen.

It is the third most frequently occurring cancer in the globe in the case of prostate cancer and has mostly happened among males. The number of fresh instances is 1.6 million, 7.1%, and the mortality rate is 3.8%, which is nearly one in twenty-five males.

In the latest research on PC they put the number of new cases, deaths and other data's which are related. The cumulative statistics are shown in Table 1.

Table 1

Statistics of cancer incidence and Mortality.

Incidence	***2017***	***2018***
Estimated New Cases	161,360	164,690
Estimated Deaths	26,730	29,430
A man will be diagnosed every…	3.3 minutes	3.2 minutes
A man will die from the disease every…	20 minutes	18 minutes

3. PROSTATE CANCER DETECTION TECHNIQUE BASED ON COMPUTER-AIDED TECHNIQUE

A. Image Processing

It segments the prostate or region of concern (ROIS) from the 2D prostate input set in the first phase of this scheme. There are different techniques of segmentation and they all have some equipment and constraints. As a consequence, (Shalaby et al., 2009) used various methods of segmentation to tackle problems and completely outline prostate tissues.

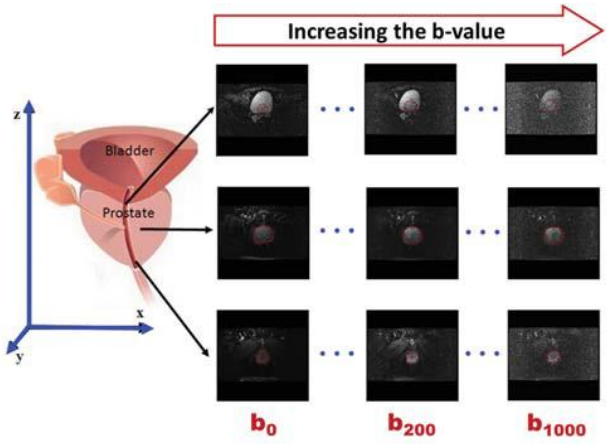

.

Figure 1. Example for DWI of prostate, (T2-MRI is the first column on the left i.e., DWI-MRI at b0)

(X. Liu et al., 2009) suggested a level-set segmentation technique on 2D DWI. In this technique, the level set motion was resulted by a rough segmentation based on data about the form of the prostate and the intensity. (X. Liu et al., 2011) created a model-based hybrid 2D/3D active form method for prostate segmentation on 3D MRI information. The diagnostic scheme based on DWI collects pictures with distinct magnetic strengths (b values). This tolerates the coefficient of obvious diffusion (ADC) and other distinguishing characteristics to be produced. It has been shown that non-cancerous regions have an average ADC greater than malignant areas. Multiple CAD systems used ADC maps to detect and diagnose prostate cancer as a discriminatory function. The resulting precision was 97.6% with 100% awareness and 95.24% specificity.

B. Convolutional Neural Network

CAD based on CNN was suggested by Reda. In this system, 3D volumes of DWI data sets collected from 40 patients at seven different b-values (100,200,400...,700 smm^{-2}) were

suggested. It begins by identifying the interest region (ROI). It automatically grows from the middle of each slice a square window of 70 / 70 pixels size. Using a generalized Gauss-Markov random field (GGMRF) model, DWI-based characteristics (ADCs) are calculated, normalized and refined. Prostate classification is performed in two phases. It uses seven CNNs in the first stage, one for each b-value to get two probabilities for each case. These CNNs ' outputs are the sophisticated ADC maps calculated for the Interest Region (ROI). The second phase combines the output probabilities with the distinct b-value and utilizes them to achieve the final diagnosis as input to an SVM with Gaussian kernel. To distinguish between benign and malignant prostates, they use two phases.

CNN is one of the deep learning network types most commonly used in the field of image analysis. They used seven CNNs in the first stage to obtain two probabilities of output for each case. The input is the sophisticated ADC volume at a certain b-value for each of these CNNs. In CNN, the first input is a 2D or 3D volume of an image, while in a traditional neural network, the weights in a CNN are somehow shared. Third, CNN includes a particular sort of layer caller pooling layer.

It comprises of four convolution layers with 32,32,64 and 64 size 5 filters in that proposed network. Two-layer, batch normalization and Relu follow each coevolutionary layer. In the second phase, for the final diagnosis, the classification utilizes an SVM with Gaussian kernel. The concept to find the hyperplane with the maximum margin between the two output classes is based on SVM. They describe a mapping feature that maps non-linearly separable information to a higher-dimensional space with linear separation.

Table 2

Result of the used CNNs at the first stage.

b-value	*Accuracy*	*Sensitivity*	*Specificity*
100 smm-2	72.5%	95.0%	50.0%
200 smm-2	77.5%	100.0%	55.0%
300 smm-2	72.5%	100.0%	45.0%
400 smm-2	75%	100.0%	50.0%
500 smm-2	70%	95.0%	45.0%
600 smm-2	75%	100.0%	50.0%
700 smm-2	72.5%	100.0%	45.0%

The result shown in Table 3 confirms the advantage of the used SVM.

Table 3

Result of SVM with Gaussian kernel

b-value	*Accuracy*	*Sensitivity*	*Specificity*	*AUC*
SVM (Gaussian Kernel)	95%	95.0%	95%	0.99
200 smm-2	82.5%	100.0%	65.0%	0.76
300 smm-2	85.5%	100.0%	70.0%	0.81
400 smm-2	85.0%	100.0%	70.0%	0.71

The scheme defines an ROI, then the ADC for that ROI is calculated and refined. The sophisticated ADC volumes are used to train a two-stage classification scheme at the distinct b- values.

C. Graph Spectral

By using graph spectral method, Du suggested some extraction technique for features. First, it extracts entire prostate. And then, in the prostate region, some statistics are calculated to determine the distinction between cancer and prostate noncancer. Statistics are mapped into Euclidean space with the help of graph spectra; technique for detecting prostate cancers. Their goal in phase 2 is to identify prostate cancer. The awareness was between 22 and 85% and the specificity was between 50 and 90%. In (B. Turkbey et al., 2009) The role of T2-weighted magnetic resonance images in prostate cancer diagnosis and therapy was examined. In CAD studies, prostate cancers such as were segmented straight into T2-weighted images.

The distinction between lesion and non-lesion region is suggested by using graph spectral method to extract certain features. First, it extracts entire prostate. In the prostate area, some statistics are calculated to distinguish between cancer and non-cancer prostate.

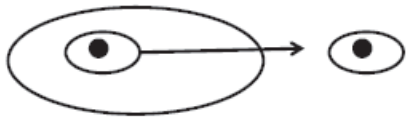

(a) Extraction type

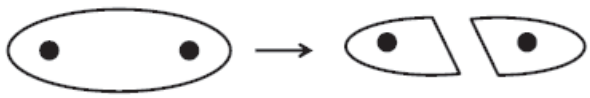

(b) Segmentation type

Figure 2. Two types of graph spectral method

In this technique, the relationship between Laplace matrix graph characteristics and spectrum or adjacency matrix is studied. There are two kinds depending on the graph spectral method solution. One is the sort of extraction; the other is the form of segmentation. Fig. 2 The two kinds are displayed. They are applied with unsupervised learning and semi-supervised learning. It depends on information geometry to search for the information relationship. This geometry can be depicted naturally by empirical chart $g = (V, E)$where nodes

V=1, 2, ..., n represent information and edges E represent information similarities. A easy concept for unsupervised graph spectral method learning is to extract in a T2-weighted picture distinct areas. Semi-supervised graph spectral method learning is about propagating the graph label. Each node begins propagating the graph's label. Each node begins to propagate its label to its neighbours, and the process is repeated until convergence takes place. The prostate can be obtained at that time. The following steps are shown for prostate extraction:

1. Different regions are needed in a picture.
2. The distinct areas are labelled.
3. The mask prostate is extracted
4. The prostate is acquired through the picture of the prostate mask and the picture weighted T2.

So, from the experiment featured can recognize cancer and noncancer, when the proper the parameter of similarity and eigenvectors were selected.

D. Microarray Dataset

The use of Learning Machines for microarray gene expression cancer information was provided by (C. Arunkumar et al., 2014) Extreme Learning Machine (ELM) solves the difficulties prevalent in traditional algorithms of inappropriate training frequency, overfitting and local minima. It was assessed on 5 benchmark information of cancer microarray gene expression i.e. for ELM's binary categorization procedure. Lung cancer, cancer of the prostate, cancer of the ovaries and CNS. Earlier to classification, feature extraction was performed with correlation coefficient. The technique operates by calculating correlation and excellent accuracy coefficient for the data types considered for Lung and Ovarian Cancers at 100 percent. The result shows that ELM performs better than conventional classification methods such as random forest, decision table, bagging and Naïve Bayes.

In many investigations, outliers are inevitable due to a variety of composite reasons ranging from the resolution of tools to data failure. The quality of the assortment and ranking of genes may affect the existence of outliers in data on the expression of microarray genes. (Z. Yang et al., 2014) classified outliers present in the expression of microarrays as structural outliers and non-structural outliers (NSOs). Structural outliers are dependent on samples or genes, while non-structural outliers have been proposed. It uses as exponentially dispersed the successive differences of well-ordered gene expressions. Both real and simulated data were used to show the effectiveness of the projected algorithm in rectifying nonstructural outliers and upgrading gene ranking/selection and fake rate control.

(Elshazly et al., 2013) addressed the dimensionality of microarray data difficulty in achieving early and accurate analysis of prostate cancer without the need for biopsy. They presented tests on different data sets to evaluate the performance of the given approach. The research results obtained show the accuracy with few other techniques of machine learning, such as decision trees and random forests.

E. Other Techniques

(Ghosh et al., 2009) suggested a model for Principal Component Analysis (PCA) and signal processing to distinguish ordinary prostate cells. For the PCA method, the amino acid sequence from cells is taken as an input sample. Coefficients of correlation were calculated between prostate cells (8 ordinaries to 8 cancer cells) and prostate cells (8 ordinaries to 8 normal). PCA research shows favourable coefficient of correlation when examining ordinary prostate databases with ordinary prostate databases. Therefore, there is a strong correlation between them indicating that they are correlated cells. But if ordinary cells indicate a adverse value out of 64 combinations, 63 combinations indicate that they are uncorrelated samples. The model is screened effectively on 8 ordinary and 8 prostate cells with Homo sapiens cancer. The model was limited to PCA alone, but not for canonical analysis.

In his article, (Singireddy et al., 2009) indicated that prostate cancer is compelled by a large degree of mysterious variation in the strength of freshly recognized disease. We understand this is one of the most prevalent cancers worldwide, finding biomarkers to effectively differentiate high-risk patient group is a basic step in growing quality of life and post-treatment survival rates.

Here the dataset was chosen with 106 samples of prostate cancer, representing different phases of prostate cancer. The goal was to acknowledge differential transcripts.

4. SUMMARY AND DISCUSSION

Table 4 summarizes the discussion of different techniques and all other techniques available for the detection of prostate cancer with the proposed algorithm, the time required for data and the accuracy of the proposed method.

Table 4

ALL TECHNICAL COMPARISON (ALGORITHMS)

SL. No.	***Algorithm***	***Time***	***Space***	***Accuracy***
1	Identifying Differentiality Expressed Transcripts	Calculations: Tophat2 and Cufflinks used genome mapping and transcriptome assembly. Differential transcripts	The dataset consisted of 106 samples of prostate cancer of various cancer stages.	The mapping rate for all the samples ranged from 80% to 99%.

SL. No.	*Algorithm*	*Time*	*Space*	*Accuracy*
		are found.		
2	Echogenicity and differential echogenicity correlation in Vitro	Every slice was stained, then interpretation followed. Calculations: system-dependent time and frequency echogenicity measures, system-independent echogenicity.	Slices of prostate tissue were obtained from specimens excised in 19 planned cases of radical prostatectomy.	The method used differential echogenicity values and Gleason score to identify cancerous and non-cancerous tissues.
3	Prostate Ultrasound Image Analysis	Calculations: Peripheral zones have been identified for each image. A size 2,538-pixel fixed region of interest has been identified. The grey scale value distribution was calculated.	The pictures were 512 * 512 pixels with 8-bit data.	Evaluated 80 percent accuracy of cancer and non-cancer cells.
4	Gene-Expression Classification of cancer by selecting features with KNN and SVM classifiers	Calculations: The analysis score for linear discrimination along with mean and SD was calculated. Euclidean distances for KNN are	The dataset includes 49 non-tumour samples and 52 prostate samples, 12,600 genes	Fisher gives 85% Relief gives 97% accuracy, SNR provides 100% accuracy, T-statistics give a 97% accuracy.
		calculated	in total.	
5	Hybrid Genetic Algorithm simulated annealing	Calculations: temperature depending on the parameter of the annealing. The probability of acceptance depends on the calculation of the individual temperature parameter for SVM, KNN, NBC and ANN.	50 Healthy and 52 samples of prostate cancer	For data on prostate cancer, HGASA's features obtained the highest classification accuracy with 88 percent accuracy on the SVM classifier.
6	Extended BRP	Calculations: Biomimetic structures, considering no, were constructed for each class. Of genes, distance, structure planar / linear. The ranking of genes was calculated on average SD.	Of the 12,600 genes, 59 were normal and 77 were cancerous	The methodology proposed yields similar or higher predictability (88% for prostate cancer)
7	Search for potential Markers for prostate cancer Diagnosis	Initially, tissues were deparaffinated, rehydrated and incubated. Protein pilot 2.0 has been used to identify and	Twenty cases of prostate tissue from ten BPH patients and ten cases of tumour node metasta	It recognized 825 non-duplicate gene products of 1420 proteins (> 95% confidence) among specimens of BPH and PCa.

SL. No.	*Algorithm*	*Time*	*Space*	*Accuracy*
		quantify proteins for iTRAQ.	sis (PCa) were investig ated.	
8	Binary Classificati on of cancer	In order to find the relationshi p between genes, Pearson product moment Correlatio n is calculated. It uses Moore-Penrose weighted matrix inverted technique.	A total of 12,600 prostat e genes were taken into account .	The method had a 81% accuracy setback for prostate cancer, but 100% for some other types.
9	Automated detdection of prostate cancer nuclei	Classificati on was based on average distance and standard deviations (SD). Other calculation s: ratio of circumfere nce, axis ratio, average level of grey	The picture s conside red were 24 bit / pixel 768 * 576 pixels.	The method works with 65.7 percent accuracy in the classificati on of objects Nucleus and Non-nucleus.
10	Population based Outlier Detection	Involved calculation s: Declaratio n of a non-negative distance vector. Used with an updated coefficient and empirical density gradient learning algorithm.	Data consist ed of 900 non-differen tial genes (DEGs) and 100 up controll ed DEGs.	The non-structural outliers were identified by the exponenti al distributio n of the phrases.
11	Graph Spectral	Calculatio n: The statistics are mapped in m dimension al Euclidean space.	The resoluti on of the graph weighte d images is 512*51 2	The accuracy is nearly 100% because it can detect the both cancerous and non-cancerous cell.

5. CONCLUSION

The above-mentioned methods indicate that a method that correctly detects prostate cancer with significant time in the early phases is still needed. The characteristics are well known worldwide, fundamental understanding of bioinformatics is needed and during the process there would be no need for expertise. NCBI openly provides a dataset that detects prostate cancer in the early phases, so it can be cured to the earliest.

ACKNOWLEDGEMENTS

We thank Professor Dr. Md. Mamunur Rashid (Dean, Faculty of ECE, Bangladesh Army University of Science and Technology) for supporting us. We gratefully thanks Bangladesh Army University of Science and Technology authority for helping us in collecting information.

REFERENCES

B. Turkbey, P. S. Albert, K. Kurdziel, and P. L. Choyke, *Imaging localized prostate cancer: current approaches and new developments*, Amer. J. Roentgenology, vol. 192, no. 6,pp. 1471-1480, Jun. 2009.

Fritz H Schr¨oder et al., "Prostate-cancer mortality at 11 years of follow-up," New England Journal of Medicine

H. Hricak, P. L. Choyke, S. C. Eberhardt, S. A. Leibel, and P. T. Scardino,"Imaging prostate cancer: a multidisciplinary perspective," Radiology, vol. 243, no.1, pp. 28–53, 2007.

J. Hugosson, S. Carlsson, G. Aus, S. Bergdahl, A. Khatami, P. Lodding, C.-G. Pihl, J. Stranne, E.Holmberg, and H. Lilja, "Mortality results from the Göteborg randomised population-based prostate-cancer screening trial," The Lancet Oncology, vol. 11, no. 8, pp. 725–732, 2010.

K. Mistry and G. Cable, "Meta-analysis of prostate specific antigen and digital rectal examination as screening tests for prostate carcinoma," The Journal of the American Board of Family Practice, vol. 16, no. 2, pp. 95–101, 2003.

M. Davis, M. Sofer, S. S. Kim, and M. S. Soloway, "The procedure of transrectal ultrasound guided biopsy of the prostate: a survey of patient preparation and biopsy technique," The Journal of Urology, vol. 167, no. 2, pp. 566–570, 2002.

M. Fuchsjäger, A. Shukla-Dave, O. Akin, J. Barentsz, and H. Hricak, "Prostate cancer imaging," Acta Radiologica, vol. 49, no. 1, pp. 107–120, 2008.

P. Vos, et al, "Automatic computer-aided detection of prostate cancer based on multiparametric magnetic resonance image analysis," Physics in medicine and biology, vol. 57, no. 6, p. 1527, 2012.

S. Dijkstra, P. Mulders, and J. Schalken, "Clinical use of novel urine and blood based prostate cancer biomarkers: a review," Clinical Biochemistry, vol. 47, no. 10–11, pp. 889–896, 2014.

S. Punwani, M. Emberton, M. Walkden, A. Sohaib, A. Freeman, H. Ahmed, C. Allen, and A. Kirkham, "Prostatic cancer surveillance following whole-gland high-intensity focused ultrasound: comparison of MR Iand prostate-specific antigen for detection of residual orr ecurrent disease," British Journal of Radiology, vol.85, no. 1014, pp. 720, 2012.

T. Tamada, et al, Apparent diffusion coefficient values in peripheral and transition zones of the prostate: comparison between normal and malignant prostatic tissues and correlation with histologic grade," Journal of Magnetic Resonance Imaging, vol. 28, no. 3, pp.720-726, 2008

T. Y. Chan and J. I. Epstein, "Patient and urologist driven second opinion of prostate needle biopsies," The Journal of Urology, vol. 174, no. 4, pp. 1390–1394,2005.

W. Du, K, Urahama, Natural image matting with membership propagation, IPSJ Trans. CVA, vol. 1, no. 1, pp. 3-11, 2009

X. Liu, M. A. Haider, and I. S. Yetik, "Unsupervised 3D prostate segmentation based on diffusion-weighted imaging MRI using active contour models with a shape prior," Journal of Electrical and Computer Engineering, vol. 2011, p. 11, 2011.

A. Madabhushi, et al, Automated detection of prostatic adenocarcinoma from high-resolution ex vivo MRI. IEEE Trans. Med. Imaging, 2005.

C.Arunkumar and Dr.S.Ramakrishnan, Binary Classification of Cancer Microarray Gene Expression Data Using Extreme Learning Machines, IEEE International Conference on Computational Intelligence and Computing Research, 978-1-4799-3975-6/14,IEEE,2014

G. Fichtinger, A. Krieger, R. C. Susil, A. Tanacs, L. L. Whitcomb, and E. Atalar, "Transrectal prostate biopsy inside closed MRI scanner with remote actuation, under real-time image guidance," in Proceedings of the 5th International Conference on Medical Image Computing and Computer-Assisted Intervention, (MICCAI'02), Toyko, Japan, September 25–28, 2002, pp. 91–98.

G. Litjens, O. debats, J. barentsz et al. Computer-aided detection of prostate cancer in MRI, IEEE. Trans. on Medical Imaging, vol. 33, no. 5, pp. 1083-1092, May 2014

Hanaa Ismail Elshazly, Abeer Mohamed Elkorany, Aboul Ella Hassanien, Ensemble-based classifiers for prostate cancer Diagnosis, Computer Engineering Conference (ICENCO), 978-1-4799-3370-9/13, IEEE, 2013

M. I. J. A. Y. Ng and Y.Weiss, On spectral clustering: Analysis and an algorithm, IEEE Trans. Patt. Anal. Mach. Intell., vol.22, no. 8, pp 888-905, 2000.

W. Du, S. Wang, A. Oto, Y. Peng, Graph-based prostrate extraction in T2-weighted images for prostate cancer detection, The 11th Internation Conference on Natural Computation and The 12th International Conference Fuzzy System and Knowledge Discovery, Aug., 2015.

X. Liu, D. Langer, M. Haider, T. Van der Kwast, A. Evans, M. Wernick, and I. Yetik, "Unsupervised segmentation of the prostate using MR images based on level set with a shape prior," in Proceedings of the 31st Annual International Conference of the IEEE Engineering in Medicine and Biology Society, (EMBC'09). Minneapolis, MN, USA, September 3–6: IEEE, 2009

Y. Artan, M. A. Haider, D. L. Langer et al, Prostate cancer localization with multispectral MRI using cost-sensitive support vector machines and conditional random fields, IEEE Trans. on Image Processing, vol. 19, no. 9, pp. 2444-2455, Sep. 2010.

Y. Gao, R. Sandhu, G. Fichtinger, and A. R. Tannenbaum, "A coupled global registration and segmentation framework with application to magnetic resonance prostate imagery," IEEE Transactions on Medical Imaging, vol. 29, pp. 1781–1794, 2010.

Zihua Yang and Zheng Rong Yang,Detection of non-structural outliers for microarray experiments, Neural Network (IJCNN), International Joint Conference,978-1-4799-5,IEEE,2014

A. Firjani, A. Elnakib, F. Khalifa, G. Gimmel'farb, M.Abou El-Ghar, A. Elmaghraby, and A. El-Baz, "A diffusion-weighted imaging based diagnostic systemfor early detection of prostate cancer, " J. Biomed. Sci.Eng., 2013.

E. Niaf, et al, Computer-aided diagnosis of prostate cancer in the peripheral zone using multiparametric MRI. Phys. Med. Biol., 2012.

Jonas Hugosson et al., "Mortality results from the g¨oteborgrandomised population-based prostate-cancer screening trial," The Lancet Oncology

Nukaga, K., Matsuda, T and Sobue, T. "Prediction of the future mortality of cancer in Japan", White Paper on cancer andstatistics 2012. [Japanese]

American Cancer Society, "Key Statistics for Prostate Cancer [Online]. Available," http://www.cancer.org/cancer/prostatecancer/about/key-statistics.html.

Cancer Org "Cancer society atlanta", (2011). [Online]. Available: http://www.cancer.org

Howlader, N. et al. (eds). "SEER cancer statistics review",1975-2010[Online]. Available: http://seer.cancer.gov/csr

Wiley Online Library, "Human prostate cancer risk factors", (2004) Available: https://onlinelibrary.wiley.com/doi/full/10.1002/cncr.20408

Wiley Online Library, "Global cancer statistics 2018: GLOBOCAN estimates of incidence and mortality worldwide for 36 cancers in 185 countries" (2018) Available: https://onlinelibrary.wiley.com/doi/full/10.3322/caac.21492